High precision tilt observation at Mt. Etna Volcano, Italy

Angelo Ferro[(1)], Salvatore Gambino[(1)], Stefano Panepinto[(2)], Giuseppe Falzone[(1)], Giuseppe Laudani[(1)] and B. Ducarme[(3)]

[(1)] *Istituto Nazionale di Geofisica e Vulcanologia, Sezione di Catania, P.zza Roma 2, 95123 Catania, Italy*

[(2)] *Dipartimento di Chimica e Fisica della Terra ed Applicazioni alle Georisorse e ai Rischi Naturali (CFTA),Università degli Studi di Palermo, Italy*

(3) *International Center for Earth tides – Catholic University of Louvain, Georges Lemaître Centre for Earth and Climate Research*

In print on Acta Geophysica

Correspondence to:

Salvatore Gambino
Istituto Nazionale di Geofisica e Vulcanologia
Sezione di Catania P.zza Roma 2, 95123 Catania, Italy
tel. number 39-95-7165800; fax number: 39-95-435801
e-mail: gambino@ct.ingv.it

Abstract

In 2007-2008, we installed on Mt. Etna two deep tilt stations using high resolution, self-leveling instruments. These installations are the result of accurate instrument tests, site selection, drilling and sensor positioning that has allowed detecting variations related to the principal diurnal and semidiurnal tides for first time on Mt. Etna using tilt data.

We analyzed the tidal effects recorded on tilt signals and we removed tidal effects from signals, thereby allowing to detect changes of about 20 nanoradians with a considerable improvement respect to the previous installation.

Tilt changes have accompanied the Mt. Etna main eruptive phases and are generally related to the rapid rise of magma and formation of dikes and eruptive fissures. However, tilt changes characterize lava fountains, earthquakes and inflation-deflation phases.

The 2008-2009 eruption represents an example of the potential of these tiltmeters providing new perspectives for highly precise monitoring of ground deformation on volcanoes.

Keywords: Tilt borehole tiltmeter, Earth tides, Mt. Etna, volcanic signals.

1. Introduction

Continuous tilt measurements are used for ground deformation monitoring in many volcanic areas and are usually used to record middle-short term eruption precursors (e.g. Toutain et al. 1992; Voight et al. 1998; Gambino 2002; 2005; Gambino et al. 2007).

Slow (weekly-monthly) tilt variations could indicate inflation caused by rising magma prior to the eruption or deflation linked to energy release following eruptions (e.g. Bonaccorso et al. 2008), while fast tilt variations (from hours to days) are related to rapid rise of magma and propagation of dikes and eruptive fissures (e.g. Bonaccorso and Gambino 1997).

Tilt changes accompany the main eruptive phases on Mt. Etna. Continuous acquisition allowed to identify eruption precursors generally related to the rapid rise of magma and formation of dikes and eruptive fissures and provided an important contribution to the analytical modeling of the volcano

sources acting during eruptions (e.g. Aloisi et al. 2003; 2006; 2009; Bonforte et al. 2009). Amplitude of these tilt variations may vary over several orders of magnitude but generally consists of several microradians; other processes such as summit crater paroxystic phases, faulting and long-term volcano/tectonic processes are generally characterized by smaller variations that may be masked by noise.

Tiltmeters are affected by various surface and temperature-related noise effects (e.g. Dzurisin, 1992) that may be related to distortion effects of the topography, air pressure, water table variations and tides but mainly to the temperature fluctuations that cause thermoelastic strain.

Mt. Etna shallow stations (about 3 meter), installed in the 90's, generally have a mean precision in the order of 0.3-0.5 microradians. Efforts to improve the performance of tiltmeters can be divided in two categories: increasing the length of the baseline to reduce the local effects and installing the instrument in a deeper hole. Levine et al. (1989) concluded that deep borehole instruments are more suited to measure tilt accurately. Bonaccorso et al. (1999), conducting an experiment on installing tiltmeters in the same hole at different depths, suggest placing the instrument at least 8-10 meters deep for volcano monitoring.

Mt. Etna tilt signal is almost free from influences of water table variations. Strong precipitation and snow melt events may cause significant increases in the ground water level that may produce evident tilt signals (e.g. Kümpel et al., 1988; 1999; Weise et al., 1999; Jahr et al., 2009). However, this effect is reduced with the water level depth (Kümpel et al., 1988) and a recent reconstruction of the Mt. Etna aquifer (Ferrara and Pappalardo, 2008) highlights that the water level is located more than 300 meters below the tilt stations.

Conversely water infiltration during and after the strong precipitation, cause tilt variation (e.g. Breitenberg, 1999; Bonaccorso et al., 1999). These episodes, though not very frequent Etna, are kept under control to avoid erroneous considerations regarding tilt variation.

In 2007-2008, we installed two new deep stations using new high resolution (<0.005 microradians) instruments, self-leveling with onboard magnetic compass. A first installation at 30 depth,

"Mascalucia" (MAS), and a second one at 10 meters "Case Bada" (CBD) have been done using the LILY Tiltmeter designed by AGI (AGI, 2005) installed in massive lava. These installations are the result of accurate instrument tests, site selection, drilling and sensor positioning in order to obtain an adequate matching of the instrument to the surrounding rocks.

A constant recorded temperature characterizes the sensors installed at MAS and CBD and recorded signals are characterized by a very low noise that have allowed detecting, for first time on Mt. Etna, signals related to the principal diurnal and semidiurnal tilt tides whose amplitude are about 0.2 microradians.

A precise tidal gravity model of Mt. Etna has been proposed for the first time by Panepinto et al., (2008). In a similar way we determined a model for tilt tides from the analysis of one year of data recorded at CBD station. Using these adjusted tidal parameters, we afterwards corrected the tilt recordings by synthetic tides. Residual signals reach a precision of 0.02 microradians with an improvement of one order of magnitude compared to the original signals.

Tilt signals related to the 2008-2009 Mt. Etna eruption represent an example of the potential of new highly precise tiltmeters.

2. Tilt network

At present, the Mt. Etna permanent tilt network (Fig. 1) comprises 13 bi-axial instruments installed in shallow bore-holes and one 80 meter long-base instrument. The borehole instruments use a high precision electrolytic bubble sensor to measure the angular movement ($\partial z/\partial x$) and each tiltmeter is composed of two perpendicular axes, named +x component and +y. The second is orthogonal to +x and a positive signal variation means uplift in the anticlockwise direction (Fig 1, Fig. 2).

The tiltmeter principle is that the bubble, suspended in the liquid-filled case, remains stationary with respect to the vertical gravity vector: when the instrument tilts, the case moves around the bubble and the electrodes sense changes of resistance as the surface covered by the conductive liquid decreases

on one side and increases on the other. A stable circuitry inside the tiltmeter converts these changes to high-level DC signals linearly proportional to angular rotation.

Eight stations were installed in the 90's in shallow boreholes at about 3 m depth and equipped with Applied Geomechanics Inc. Mod 722 and Mod 510 tiltmeters. These kinds of tiltmeters have a nominal precision respectively of 0.1 and 0.01 microradians. However, the real precision is affected by environmental noise mainly due to temperature effects. At a depth of a few meters, the thermoelastic effects may produce a noise both in seasonal and daily variations (e.g. Wyatt 1988; Dzurisin 1992) so that the instrumental precision is generally of the order of 0.5 microradians.

In 1997, a long-baseline instrument comprising two 80 m long orthogonal tubes filled with mercury, was positioned along two tunnels, at the volcanological observatory of Pizzi Deneri (PDN), located 2850 m a.s.l. (Bonaccorso et al. 2004). This device shows a low temperature noise that provides a precision of about 0.1 microradians.

In recent years, we installed two new deep stations using new high resolution (< 5 nanoradians) instruments, self-levelling with onboard magnetic compass (the LILY Self-Leveling Borehole Tiltmeter designed by Applied Geomechanics). The tiltmeter (51 mm diameter and 915 mm long) have been installed in uncased holes with internal diameters of about 100 mm.

A first installation was made at 30 m depth (MAS), 20 km far from Mt. Etna’s summit; the second one (CBD) is closer to the volcano summit, 1500 m a.s.l. and is 10 m deep (Fig. 1). Between 2009 and 2010 two more stations were installed (MSP and MGL in fig. 1).The instruments have been positioned inside massive lavas layers and afterward covered by sand. (for more details see AGI, 2005). Data acquisition is programmed for 96 data/day sampling (1 sample every 15 minutes) and includes acquisition of the two tilt components, air and ground temperatures, and instrumental control parameters.

Owing to their depth, the new tiltmeters are almost unaffected by instrumental noise due to in situ temperature effects and the only evident signal is linked to the tidal signal, which is affected by

tilt/strain coupling effects and crustal inhomogeneities (Harrison and Herbst, 1977). This tidal signal is hiding the onset of geophysical signals due to volcanic activity and has to be suppressed.

3.0 Tilt associated with Mt. Etna eruptive activity

Mt Etna is a basaltic volcano situated on the eastern coast of Sicily and is one of the most active volcanoes in the world. The volcanic edifice has a basal diameter of about 40 km, is just over 3200 m high and has four active summit craters.

Activity on Mt. Etna may be divided into two types, lateral flank eruptions occurring along fracture systems and persistent activity that comprises phases of degassing alternating with Strombolian activity, which may occasionally evolve into lava fountains and effusive activity.

Tilt changes recorded by the INGV-CT permanent network have accompanied all the main eruptive phases on Mt. Etna since 1981.

Tilt recording plays a fundamental role in real time monitoring because it provides a signal able to detect ground deformation changes with high precision. At Mt. Etna, tiltmeter excelled at detecting rapid and sharp variation such as the ones recorded during intrusions and eruptive fissure propagation (e.g. Aloisi et al. 2003; 2006; 2009).

In figure 2 we report the location of the magma intrusion source for the eruptions of last 30 years at Mt. Etna (1981, 1989, 1991-1993, 2001, 2002 and 2008-2009). These sources modeled using tilt and GPS data are not very deep (between 2000 m b.s.l. to 1000 m a.s.l.). The intrusive phases caused on most stations tilt changes with an amplitude that is related to source-station distance; for example the 2002 case showed a very high variation at PDN and MNR but a small one at CDV (fig. 3a).

During the 2002 eruption a dike intrusion propagated laterally (red arrow in fig. 3b) from the summit craters to the eruptive fractures (Andronico et al., 2005) and was accompanied by seismicity (Fig. 3b). Tilt vector map showed a general uplift toward the intrusion area (fig. 3b). Tilt vectors are turned towards the line of tract of lava flow evidencing an extension process due to the magma

intrusion which propagated laterally from summit craters along the Mt. Etna NE rift (Aloisi et al., 2003).

Small but detectable tilt was also recorded on Mt. Etna during strong crater paroxystic phases (Bonaccorso, 2006) and faulting earthquakes (Alparone and Gambino, 2003; Bonforte et al., 2007); moreover evident long-term inflation/deflation phases have been recognized (Allard et al., 2006; Gambino and Guglielmino, 2008).

However, an improvement of the signal-to-noise ratio may greatly improve the ground deformation detection on Mt. Etna highlighting less energetic processes that are currently masked by background noise.

4.0 Tides

Gravitational attraction of the Sun and Moon modify the gravity vector and deform the Earth's shape producing tides with different periods. Gravity changes, surface displacements, strain and tilt are different observable components of the tidal phenomenon. It is important to measure the Earth's tides because it is not only a direct way to a better knowledge of the internal structure of the Earth, but also a useful tool in the research on major natural disasters, such as earthquakes and volcanic eruptions.

The stress variations induced by the tidal forces in the crust do not exceed 10^3Pa and might seem too small to trigger earthquakes and volcanism. Nevertheless, the idea that tides may influence these geophysical events has been discussed since 1930, when an interesting earthquake sequence was observed during an earthquake swarm east of Ito on the Izu Peninsula, central Japan and it is still debated if tidal stress changes as low as a few kPa may significantly affect the eruptive behavior of volcanoes (e.g. Sparks 1981; Kasahara 2002).

4.1 Earth tide analysis

We performed an Earth tide analysis of the CBD tiltmeter data set may 2009 – april 2010 using the software package ETERNA 3.4 (Wenzel, 1996) with the Tamura tidal potential and Pertsev numerical filter. The adjusted tidal parameters for the N220.5E and the N130.5E components are given in Tables 1 and 2 respectively. The standard deviation of weight unit for the two components are respectively 3.7 and 4.8 mas (18 and 23 nanoradians). The precision is better than 2% or 0.2mas (1nrad) on the amplitude of the main tidal wave M2.

The tidal amplitude factor γ is defined as the ratio between the observed and the astronomical amplitudes of the considered tidal wave. Tidal models based on an elastic Earth predict γ values close to 0.7 (Melchior, 1983). The analysis provides γ values between 0.5 and 0.8 for the main tidal components, in reasonable agreement with the theory considering the local condition. The depth of the borehole is not completely protecting the instrument again the thermal strain propagating from the surface to depth larger than 50m and responsible of the so called tilt/strain coupling (Harrison and Herbst, 1977). Tilt measurements are very sensitive to discontinuities in the crust as well as local topography and the volcano edifice is very heterogeneous and is a huge topographic anomaly (Harrison, 1976). It should be necessary to build a finite element model of the volcano to compute the different effects (Gebauer et al., 2009). Perturbations of thermal origin are confirmed by the high γ value of the meteorological wave S1, corresponding to the solar period of 24h. As a matter of fact its amplitude is of the order of 2 mas (0.01microrad) and is thus one order of magnitude lower than the volcanic signals (see Figure 7). The phase delays α (a few degrees) are defined as differences between the observed phase and the astronomical one. The α values can be large for the diurnal waves but are always below 10° for the semidiurnal ones. These values indicate that the possible error of azimuth of measurement is acceptable for investigations of tilting of volcano edifice. Delay of tidal waves is an result of interaction of tidal waves with discontinuities in the crust, but it is puzzling that the phase delays are always negative (lags).

These phase lags are perhaps linked to residual magnetization of lava flow that may have influenced the onboard magnetic compass; in fact directions of residual magnetization of Mt. Etna lava flows may vary by several degrees for magma erupted during the last centuries (Incoronato and Del Negro 2004).

Figure 4 shows observed and theoretical signals; the two signals have a very similar shape, confirming the stability of the instrument and the good response of the sensor to tidal deformation, as already represented by the tidal analyses. In figure 5 the main tidal constituents, i.e. semidiurnal and diurnal, are recognized by spectral analysis and only weak spectral power is left after correction using the tidal model. The accuracy of the tidal model can be deduced from the residues. It is of the order of 5mas (0.025µrad) or 10% of the tidal tilt. In any case perfect reduction of tidal signals is not required as the magnitude of tilt signals resulting from volcano activity are at least one order of magnitude larger.

5.0 Removing the tide component; the 2008-2009 eruption case.

The reduction of tidal tilt (or gravity) signals is important in order to detect tectonic-volcanic deformation (e.g. Battaglia and Hill, 2009; Jahr et al., 2009).

In figure 6 we report the two tilt components of CBD corrected by the modelled tides. The residual signal is able to appreciate changes in the order of 0.02-0.03 microradians and the records of the 2008-2009 eruption represents an example of the potential of the high precision tiltmeter data. The instrumentation was able to detect co-seismic (i.e. main volcano earthquakes and seismic swarms), co-explosive (i.e. summit crater paroxystic phases) and eruptive (i.e. intrusion preceding the eruptions) events.

In figure 7 we report the tide-removed data of the two CBD components, from the 13 days before the beginning of the 2008-2009 eruption. Under these conditions, the instrument seems to record a variation of 0.1–0.15 microradians during the 20 hours preceding the onset of the 2008-2009 eruption (Fig. 7).

6.0. Discussion and conclusions

Continuous tilt measurements are generally used on Mt Etna to record middle-short term eruption possible precursors.

Tilt associated with intrusive and fracturing mechanisms may vary over several orders of magnitude but generally consists of several microradians; other processes such as summit crater paroxystic phases, faulting and long-term volcano/tectonic processes are generally characterized by smaller variations that may be masked by noise.

Tiltmeters are affected by various surface and temperature-related noise effects (e.g. Dzurisin 1992) that may be related to distortion effects of the topography, air pressure, water table variations and tides but mainly to the temperature fluctuations that cause thermoelastic strain.

The installation of a tilt sensor in a deep hole is considered the most suitable way to measure tilt accurately (Levine et al. 1989) and effectively we obtained high signal-to-noise signals from the recent installation at Mt. Etna containing only the tide components. The increased depth of measurements has practically reduced the bias of meteorological factors on measurements.

Though tilt resulting from Earth tides is small, some authors suggest that tidal stress changes may affect the eruptive behavior of volcanoes. Indeed, though small, we evidenced that amplitude of the tilt variations is in the order of 0.1-0.2 microradians for the diurnal and semidiurnal tidal component in the Mt. Etna area.

We calculated for CBD a precise tidal tilt model. Using these modeled (from analyses) tides, we removed tidal effects from signals of CBD and residual signals is able to appreciate changes in the order of 0.02-0.03 microradians with an improvement of one order of magnitude compared to the previous shallower data.

The beginning of the 2008-2009 eruption represents an example of the potential of these signals.

On 13 May 2008, an eruption started on Mt. Etna; magma intrusion was accompanied by a violent seismic swarm and marked ground deformation was recorded at permanent tilt and GPS stations.

Aloisi et al. (2009) showed that the 2008 intrusion was characterized by an intrusive mechanism that started from the central conduit at 1600 meters below the ground, breaking off towards the east and up.

Tide corrected residues show better a small anomaly (0.1-0.2 microradians) during the 20 hours before the onset of the 2008-2009 eruption more evident on the N220.5E component trend.

It is not easy to give an explanation for this phenomenon; the effects of this process still seem small and moreover we have not found data, which might help us, on other devices installed on Mt. Etna. However the presence of more tilt stations of higher precision (Mt. Etna has now four stations) will allow to improve our knowledge on less energetic processes that could be very important inside the volcano activity.

Acknowledgements

We want to thanks the two anonymous referees for their reviews leading to substantial improvements of the manuscript. We are indebted with Prof. Letterio Villari who promoted the Mt. Etna tilt network. We also thanks Orazio Campisi and Benedetto Saraceno for their support to the network functionality.

References

AGI (2005), LILY Self-Leveling Borehole Tiltmeter User's Manual, Applied Geomechanics Inc. Manual No. B-05-1003, Rev. A. http://www.geomechanics.com/dspproduct.cfm?prid=88.

Allard, P., B. Behncke, S., D'Amico, M., Neri and S. Gambino (2006), Mount Etna 1993–2005: Anatomy of an evolving eruptive cycle. *Earth Science Review*, **78**, 85-114.

Aloisi, M., A. Bonaccorso, S., Gambino, M., Mattia, and G. Puglisi (2003), Etna 2002 eruption imaged from continuous tilt and GPS data. *Geophys. Res. Lett.*, **30**, 23, 2214 10.1029/2003GL018896.

Aloisi, M., A. Bonaccorso, and S. Gambino (2006), Imaging compositive dike propagation (Etna, 2002 case). *J. Geophys. Res.*, **111**, B06404, doi: 10.1029/2005JB003908.

Aloisi, M., A. Bonaccorso, F., Cannavò, S., Gambino, M., Mattia, G., Puglisi, and E., Boschi (2009), A new dyke intrusion style for the Mount Etna May 2008 eruption modelled through continuous tilt and GPS data. *Terra Nova*, **21**, 316–321.

Alparone, S.and S. Gambino (2003), High precision locations of multiplets on south-eastern flank of Mt. Etna (Italy): reconstruction of fault plan geometry. *Phys. Earth Plan. Int.* **135**, 281-289.

Andronico D., Branca S., Calvari S., Burton M., Caltabiano T., Corsaro R.A., Del Carlo P., Garfì G., Lodato L., Miraglia L., Muré F., Neri M., Pecora E., Pompilio M., Salerno G. and L. Spampinato (2005), A multi-disciplinary study of the 2002-03 Etna eruption: insights into a complex plumbing system. *Bull. of Volcanology*, **67,** 314-330.

Battaglia M. and D.P. Hill (2009), Analytical modeling of gravity changes and crustal deformation at volcanoes: The Long Valley caldera, California, case study *Tectonophysics*, **471,** pp. 45-57.

Bonaccorso A. and S. Gambino (1997), Impulsive tilt variations at Mount Etna Volcano (1990-93). *Tectonophisics*, **270** pp. 115-125.

Bonaccorso A., G. Falzone and S. Gambino (1999), An Investigation into Shallow Borehole Tiltmeters. *Geophys. Res. Lett*. **26**, 11, pp. 1637-1640.

Bonaccorso A., O. Campisi, G. Falzone and S. Gambino (2004), Continuous tilt monitoring: a lesson from 20 years experience at Mt. Etna, Monograph of American Geophysical Union "*Etna Volcano Laboratory*", Calvari, S., Bonaccorso, A., Coltelli, M., Del Negro C. & Falsaperla S., eds, pp. 307-320.

Bonaccorso A. (2006), Explosive activity at Mt. Etna summit craters and source modeling by using high-precision continuous tilt. *J. Volc. Geotherm. Res*., **158**, 221-234.

Bonaccorso A., S. Gambino, F. Guglielmino, M. Mattia, G. Puglisi and E. Boschi (2008), Stromboli 2007 eruption: Deflation modeling to infer shallow-intermediate plumbing system, *Geophys. Res. Lett*., **35**, L06311, doi:10.1029/2007GL032921.

Bonforte A., S. Gambino, F. Guglielmino, F. Obrizzo, M. Palano and G. Puglisi (2007), Ground deformation modelling of flank dynamics prior to the 2002 eruption of Mt. Etna. *Bull. Volc*., **69**, 757-768.

Bonforte A., S. Gambino and M. Neri (2009), Intrusion of eccentric dikes: The case of the 2001 eruption and its role in the dynamics of Mt. Etna volcano. *Tectonophysics*, **471**, 1-2, 78-86.

Dzurisin, D. (1992), Electronic tiltmeters for volcano monitoring : lessons from Mount St. Helens, **in** Monitoring volcanoes: techniques and strategies by the staff of the Cascades observatory, 1980-90, Ewert, J.W., and D.A. Swanson, Eds, U.S.G.S. Book, 69-83.

Ferrara V. and G. Pappalardo (2008) The Hydrogeological map of the Etna volcanic massif as useful tool for groundwater resource management. *Italian Journal of Engineering Geology and Environment*, **1**, 77-89

Gambino S. (2002), Coseismic and aseismic tilt variations on Mount Etna. *Pure Appl. Geophys*. **159**, 2751-2762.

Gambino, S. (2005), Air and permafrost temperature at Mt. Melbourne (1989-1998). *Antarctic Science*, **17**, 151-152.

Gambino S., O., Campisi, G., Falzone, A. Ferro, F. Guglielmino, G. Laudani, and B. Saraceno (2007), Tilt measurements at Vulcano Island. *Annals of Geophysics*, **50**, 233-247.

Gambino, S. and F. Guglielmino (2008), Ground deformation induced by geothermal processes: a model for La Fossa Crater (Vulcano Island, Italy), J. Geophys. Res., **113**, B07402, 10.1029/2007JB005016.

Gebauer, A., Kroner, C. and T. Jahr (2009), The influence of topographic and lithologic features on horizontal deformations, *Geophys. J. Int.*, **177**, 586-602.

Harrison, J.C. (1976), Cavity and topographic effects in tilt and strain measurements, *J. Geophys. Res.*, **81**, 319-328.

Harrison, J.C. and K. Herbst (1977), Thermoelastic strains and tilt revisited, *Geophys. Res. Lett.*, **4** (11), 535-537.

Incoronato A. and C., Del Negro (2004), Magnetic Stratigraphy Procedures at Etna. Monograph of American Geophysical Union “Etna Volcano Laboratory”, Calvari, S., Bonaccorso, A., Coltelli, M., Del Negro C. & Falsaperla S., eds, 263-271.

Jahr, T., G. Jentzsch, and A. Weise (2009), Natural and man-made induced hydrological signals, detected by high resolution tilt observations at the Geodynamic Observatory Moxa/Germany. *Journal of Geodynamics*, **48**, 126-131.

Kasahara, J. (2002), Tides, earthquakes, and volcanoes, *Science*, **297**, 348–349.

Kümpel H.J., J.A., Peters and D.R. Bower (1988), Nontidal tilt and water-table variations in aseismically active region in Quebec, Canada. *Tectonophisics*, **152** pp. 253-265.

Kümpel, H.J., G. Grecksch, K, Lehmann, D. Rebscher and K.C. Schulze (1999), Studies of in situ pore pressure fluctuations at various scales. *Oil and Gas Science and Technology—Review* IFP **54**, 679–688.

Levine J., C. Meertens and R. Busby (1989), Tilt observations using borehole tiltmeters 1. Analysis of tidal and secular tilt. *J. Geoph. Res*., **94**, 574-586.

Melchior P. (1983), The tides of the Planet Earth. 2nd Edition, *Pergamo Press*, *Oxford*, 641pp.

Panepinto S., F. Greco, D. Luzio and B. Ducarme (2008), Tidal gravity observations at Mt. Etna and Stromboli: results concerning the modeled and observed tidal factors. *Ann. Geoph*., **51**, 51-65.

Sparks, R. S. J. (1981), Triggering of volcanic eruptions by Earth tides, *Nature*, **290**, 448.

Toutain, J.P., P. Bachèlery, J.L. Blum, J.L. Cheminèe, H. Delorme, L. Fontaine, P. Kowalski, and P. Taochy (1992), Real-time monitoring of vertical ground deformations during eruptions at Piton de la Fournaise, *Geophys. Res. Lett*., **19**, 553-556.

Voight, B., R.P. Hoblitt, A.B. Clarke, A.B. Lockhart, A.D. Miller, L. Lynch, and J. McMahon (1998), Remarkable cyclic ground deformation monitored in real-time on Montserrat, and its use in eruption forecasting *Geophys. Res. Lett*., **25**, 3405-3408.

Weise, A., G. Jentzsch, A. Kiviniemi and J. Kääriäinen (1999), Comparison of long-period tilt measurements: results from the two clinometric stations Metsähovi and Lohja, Finland. *Geodynamics* **27**, 237–257.

Wenzel, H.G. (1996), The nanogal software: Earth tide data processing package ETERNA 3.3. *Bull. d'Inf. Marées Terr.* **124**, 9425–9439.

Wyatt, F. (1988), Measurements of coseismic deformation in Southern California: 1972-1982, *J. Geophys. Res.*, **93**, 7923-7942.

Captions

Tab1. Tidal analysis results of Eterna34 software package for CBD +x component (220.5° azimuth angle).Adjusted tidal parameters of the main tidal waves: γ amplitude factor, ε_γ standard deviation, α phase delay, ε_α standard deviation.1mas=4.848 nanoradians

Tab2. Tidal analysis results of Eterna34 software package for CBD +y component (130.5° azimuth angle). Adjusted tidal parameters of the main tidal waves: γ amplitude factor, ε_γ standard deviation, α phase difference delay, ε_α standard deviation. 1mas=4.848 nanoradians

Fig. 1. Mt Etna permanent tilt network (A) and general scheme of the bore-hole tiltmeter installation (B).

Fig. 2. Map showing the eruptive dike intrusive sources obtained by modeling tilt and GPS ground deformation data (see text for details).

Fig. 3. Tilt signals recorded between 26th and 29th October 2002 (A). EC10 and MDZ recorded small variations (1-5 microrad) that are not visible at this scale. SPC was not functioning. Tilt vectors and seismicity recorded during the 2002 Nord-Est intrusion (B). The two PDN tilt vectors (1 and 2) are due to the change of the relative position station-intrusion during the process (see Aloisi et al., 2006)

Fig. 4. Example of signal recorded at N220.5E +x component of CBD station and N276.E +x component of MAS and the corresponding modeled tilt signal. The CBD small drift effect after 2008/05/04 is probably linked to a thermoelastic effect. Borehole temperature has also been reported.

Fig. 5. Superposition of signals spectra for the 130.5 tilt component of CBD station. The black curve represents the original signal after removing of the instrumental drift by PERTZEV59 numerical filter (see Eterna34 for further information). The grey trace represents the obtained residues after tidal correction. The picture clearly shows on the one hand very sharp peaks on the principal tidal wavegroups of the tilt

recording while, on the other hand, a well defined tidal correction obtained by using the local adjusted tidal parameters coming from the executed analysis (see text for explanation).

Fig. 6. Residual signal obtained by removing modeled tidal tilt from recorded data for the N220E CBD component.

Fig. 7. Filtered signals of the two components of CBD between 1-13 May 2008. We evidenced the different processes linked to the variations recorded: co-seismic (i.e. main volcano earthquakes and seismic swarms), co-explosive events (i.e. summit crater paroxystic phases), teleseismic events (e.g. the M=8.0 Sichuan earthquake on 12 May) and eruptive (i.e. intrusion preceding the eruptions). Hole temperature has also been reported.

Table 1. Adjusted tidal parameters of the main tidal waves – CBD X component (220.5° azimuth angle)
γ amplitude factor and ε_γ standard deviation, α phase delay and ε_α standard deviation

wave	group limits		Theoretical Amplitude	Tidal parameters	
	From [cpd]	To [cpd]	[mas]	γ ε_γ	$\alpha(°)$ $\varepsilon_\alpha(°)$
O1	0.921941	0.940487	2.880	0.58777	-30.1
				±.05821	±5.7
S1*	0.999853	1.000147	0.032	43.2927	-127.1
				±8.5119	±11.2
K1	1.001625	1.011099	4.051	0.69559	-1.6
				±.04254	±3.5
N2	1.888387	1.906462	1.912	0.78957	-4.7
				±.04472	±3.2
M2	1.923766	1.942753	9.987	0.76754	-4.2
				±.00878	±0.6
S2	1.991787	2.002885	4.646	0.83629	-7.4
				±.01860	±1.2

* meteorological wave

Table 2. Adjusted tidal parameters of the main tidal waves – CBD Y component (130.5° azimuth angle).
γ amplitude factor and ε_γ standard deviation, α phase delay and ε_α standard deviation

wave	group limits		theoretical amplitude	tidal parameters	
	From [cpd]	To [cpd]	[mas]	γ ε_γ	$\alpha(°)$ $\varepsilon_\alpha(°)$
O1	0.921941	0.940487	3.219	0.82781	-4.9
				±.05456	±3.8
S1*	0.999853	1.000147	0.035	72.2329	-5.5
				±8.0138	±8.3
K1	1.001625	1.011099	4.527	0.83328	-23.3
				±.04010	±2.8
N2	1.888387	1.906462	2.053	0.48753	-10.9
				±.06023	±3.2
M2	1.923766	1.942753	10.723	0.47676	-2.8
				±.01221	±1.4
S2	1.991787	2.002885	4.989	0.59005	-10.3
				±.02582	±2.5

* meteorological wave

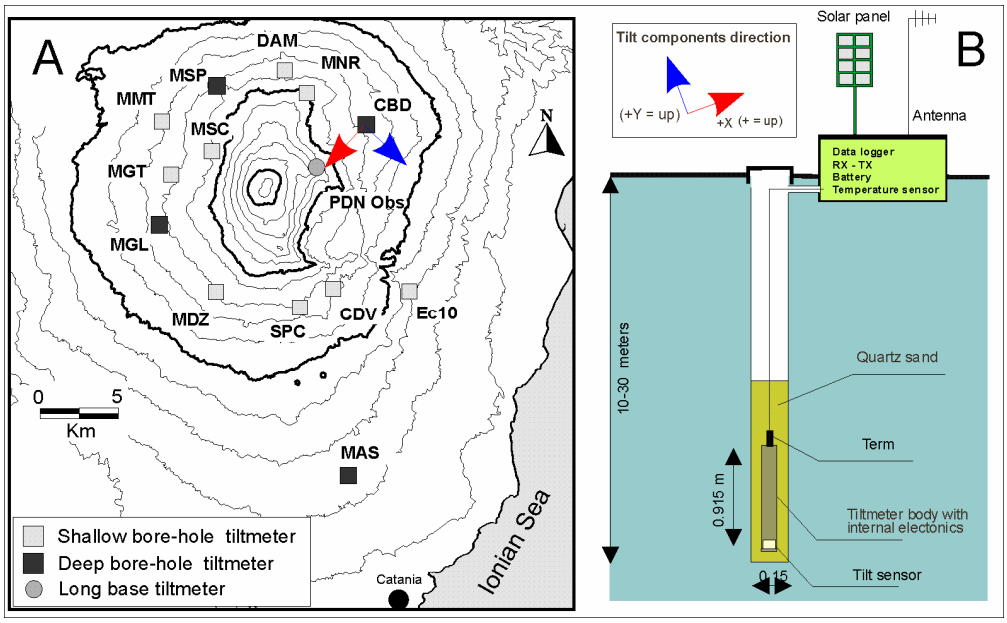
A
DAM
MNR
MSP
MMT
CBD
MSC
MGT
PDN Obs
MGL
MDZ
SPC
CDV
Ec10
0
5
Km
MAS
Catania
Ionian Sea
N
Shallow bore-hole tiltmeter
Deep bore-hole tiltmeter
Long base tiltmeter
Tilt components direction
(+Y = up)
+X (+ = up)
Solar panel
B
Antenna
Data logger
RX - TX
Battery
Temperature sensor
10-30 meters
Quartz sand
Term
0.915 m
Tiltmeter body with internal electonics
Tilt sensor
0.15

Fig. 1

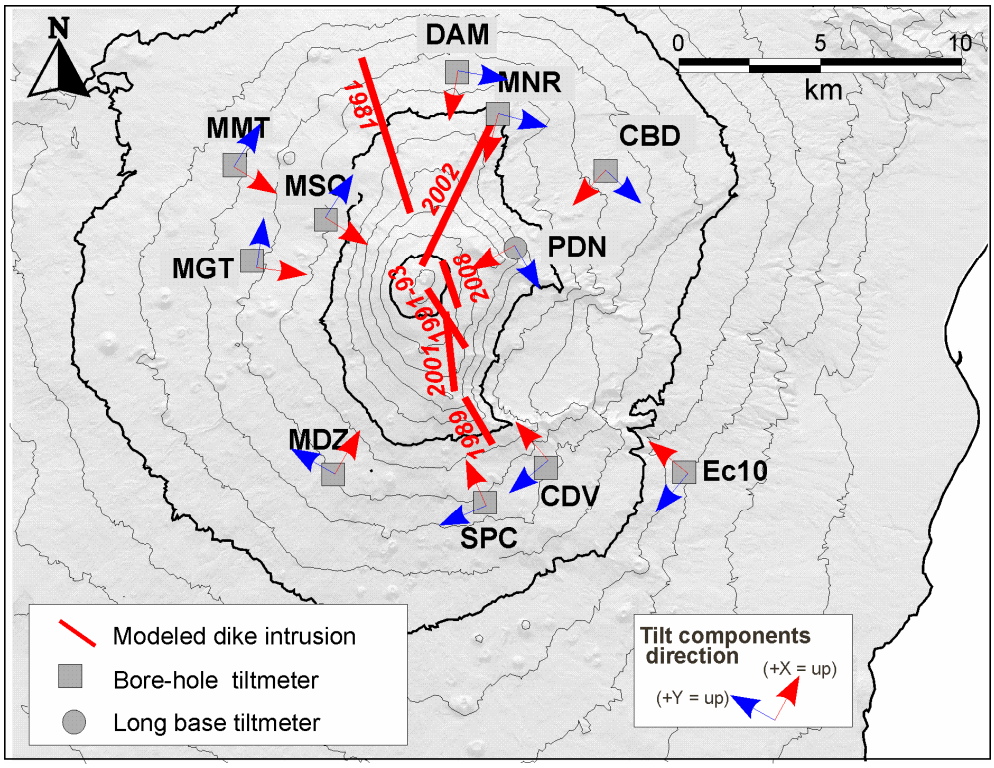
N
DAM
MNR
0
5
10
km
MMT
1987
CBD
MSC
2002
PDN
MGT
2008
1996-97
2001
1989
MDZ
Ec10
CDV
SPC
Modeled dike intrusion
Bore-hole tiltmeter
Long base tiltmeter
Tilt components direction
(+X = up)
(+Y = up)

Fig. 2.

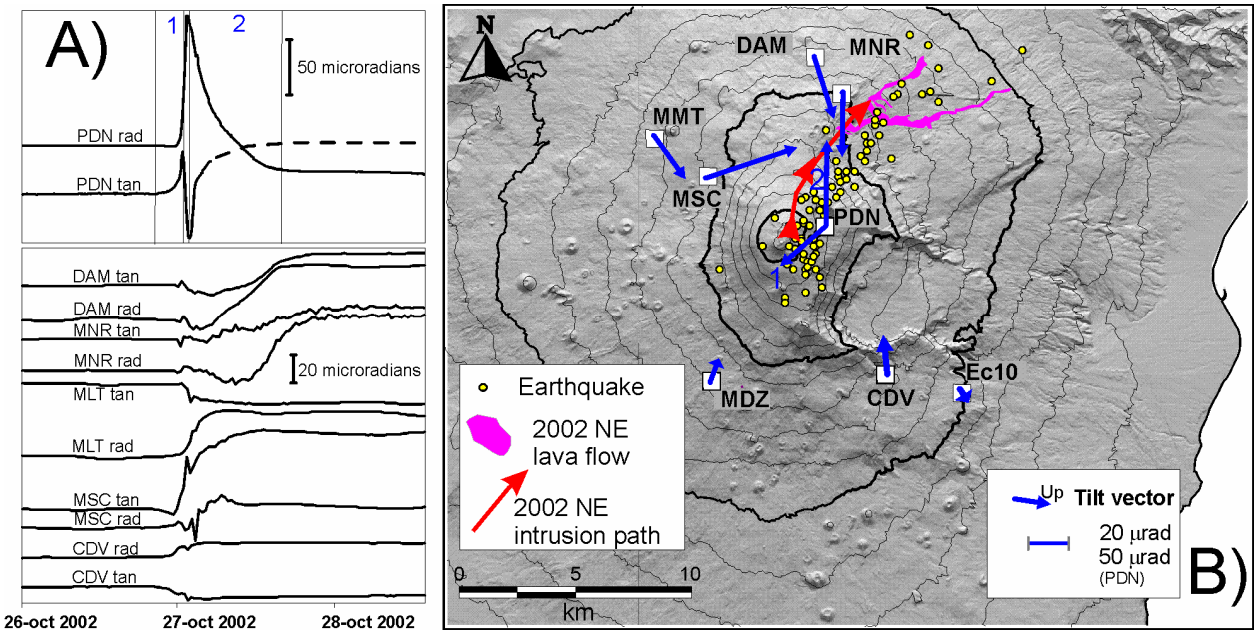
A)
1
2
50 microradians
PDN rad
PDN tan
DAM tan
DAM rad
MNR tan
MNR rad
20 microradians
MLT tan
MLT rad
MSC tan
MSC rad
CDV rad
CDV tan
26-oct 2002
27-oct 2002
28-oct 2002
N
DAM
MNR
MMT
MSC
PDN
MDZ
CDV
Ec10
Earthquake
2002 NE lava flow
2002 NE intrusion path
0
5
10
km
Up
Tilt vector
20 μrad
50 μrad
(PDN)
B)

Fig. 3

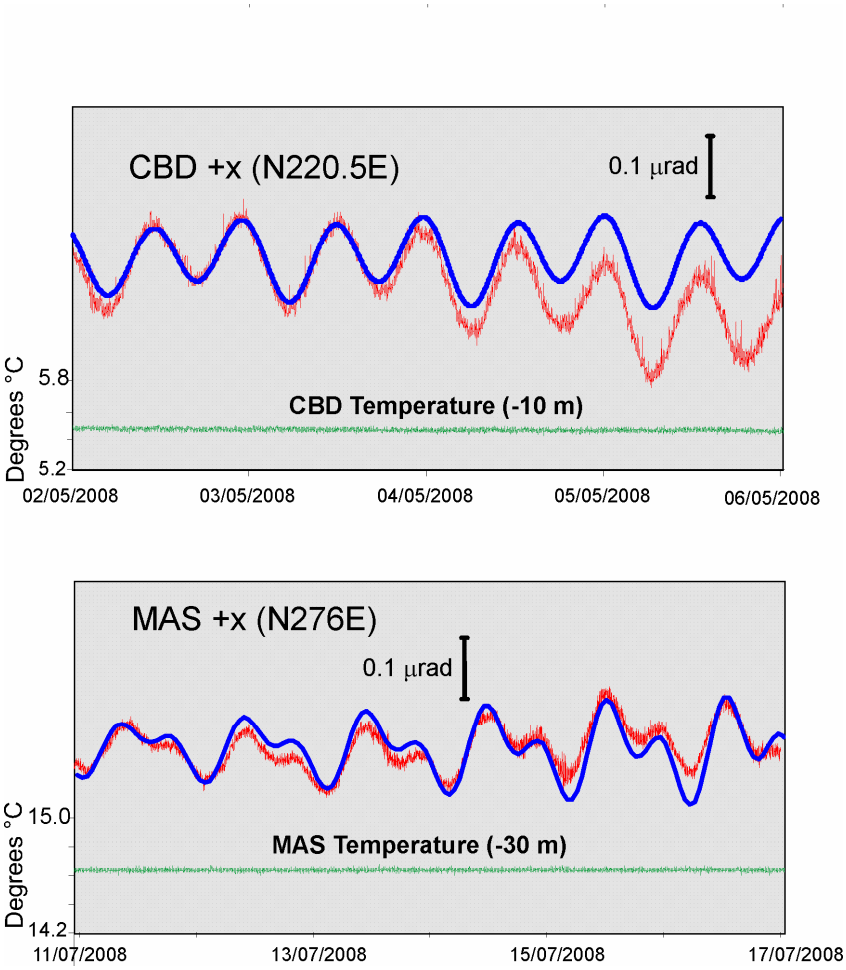
CBD +x (N220.5E)
0.1 μrad
Degrees °C
5.8
5.2
CBD Temperature (-10 m)
02/05/2008
03/05/2008
04/05/2008
05/05/2008
06/05/2008
MAS +x (N276E)
0.1 μrad
Degrees °C
15.0
14.2
MAS Temperature (-30 m)
11/07/2008
13/07/2008
15/07/2008
17/07/2008

Fig.4

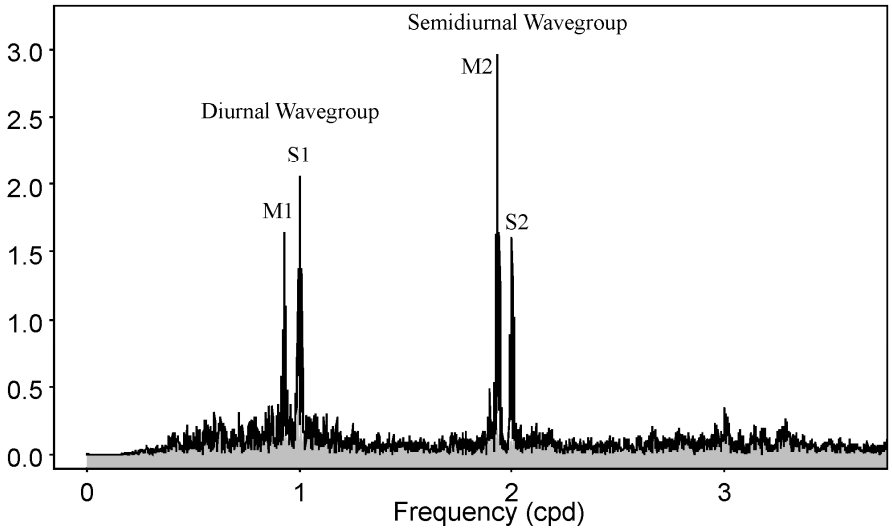
Semidiurnal Wavegroup
M2
Diurnal Wavegroup
S1
M1
S2
3.0
2.5
2.0
1.5
1.0
0.5
0.0
0
1
2
3
Frequency (cpd)

Fig. 5

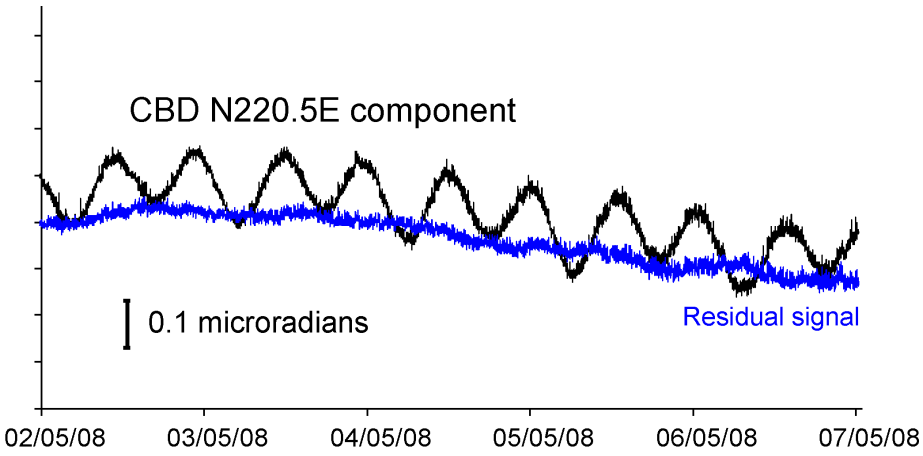
CBD N220.5E component
0.1 microradians
Residual signal
02/05/08
03/05/08
04/05/08
05/05/08
06/05/08
07/05/08

Fig 6

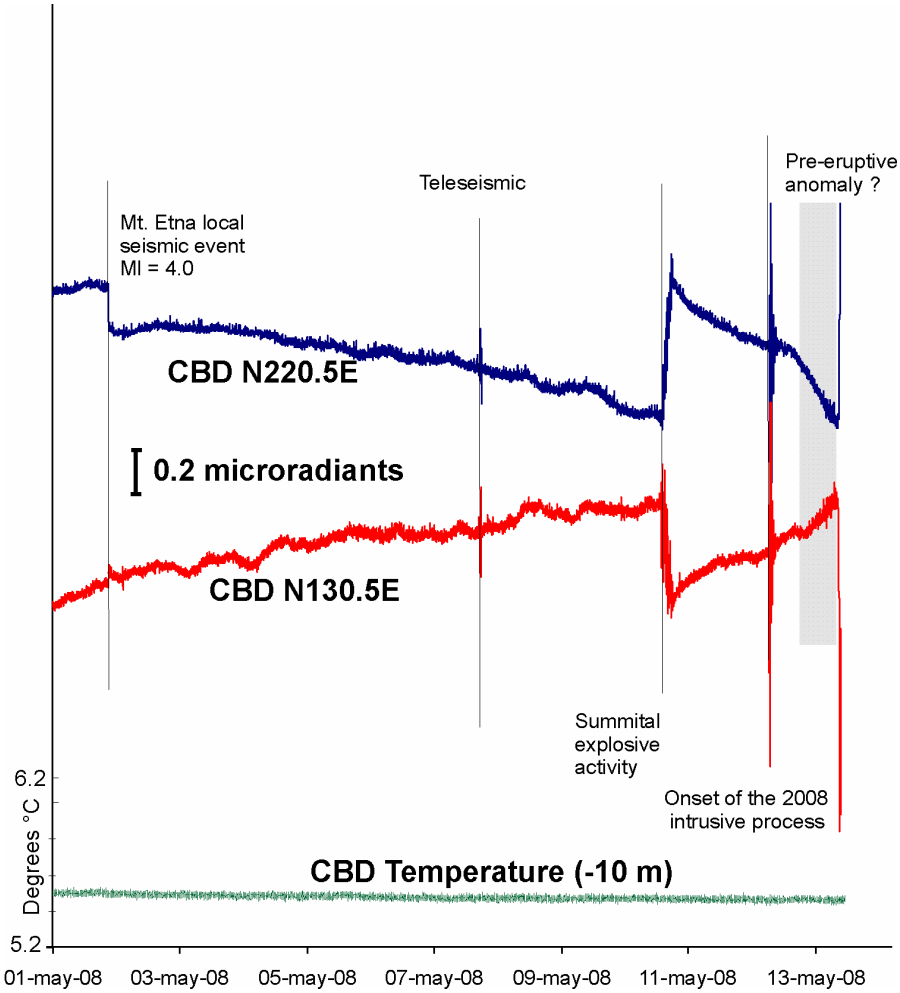
Mt. Etna local
seismic event
Ml = 4.0
Teleseismic
Pre-eruptive
anomaly ?
CBD N220.5E
0.2 microradiants
CBD N130.5E
Summital
explosive
activity
Onset of the 2008
intrusive process
CBD Temperature (-10 m)
Degrees °C
6.2
5.2
01-may-08
03-may-08
05-may-08
07-may-08
09-may-08
11-may-08
13-may-08

Fig. 7